# ENHANCED SPIRAL DYNAMIC ALGORITHM WITH APPLICATION TO INDUCTION MOTOR PARAMETERS IDENTIFICATION

EL-GHALIA BOUDISSA<sup>1</sup>, MOHAMED BOUNEKHLA<sup>1</sup>, FATIHA HABBI<sup>1</sup>

Keywords: Spiral dynamic algorithm; Meta-heuristic; Induction machine; Identification; Spiral radius; Rotational angle.

The spiral dynamic algorithm (SDA) is a metaheuristic characterized by the setting of parameters (spiral radius and rotational angle). The drawback of all meta-heuristic methods is the premature convergence, which occurs when a trade-off between exploitation and exploration is not maintained. SDA provides a good exploitation phase because all points are attracted to the best solution. But the exploration phase is poor when the spiral parameters are set to constant values during the whole search process. To improve SDA performance and circumvent premature convergence, this paper proposes an enhanced SDA in which the parameter settings vary simultaneously according to nonlinear functions. The effectiveness of the enhanced SDA algorithm (ESDA) was proven by identifying the electrical and mechanical induction motor (IM) parameters. This is achieved using the reference model method, in which the estimated parameters correspond to the minimum of the objective function. A comparison is established between the ESDA, SDAs, genetic algorithm (GA), and particle swarm optimization (PSO). The developed program and the estimation approach are tested using simulated and measured data from an IM (1.5 kW).

## 1. INTRODUCTION

Optimization methods have attracted the attention of many researchers for solving many problems in various broad fields. In general, the deterministic methods converge to a local minimum [1]. Fortunately, metaheuristics are a technique for overcoming the drawbacks of these methods. They intend to be suitable for global optimization [2] due to their random nature, allowing a jump out of local minima. The meta-heuristic techniques such as balanced aquila optimiser (BAO) [3], artificial ecosystem-based optimisation (AEO) algorithm [4], genetic algorithm (GA) [5], firefly (FA) [6], marine predators optimizer (MPO) [7], particle swarm optimization (PSO) [8], Dragonfly algorithm (DA) [9], and spiral optimization technique [10] have led to its application to optimization problems of different engineering areas.

This paper focuses on the spiral dynamic algorithm (SDA), which is inspired by spiral phenomena in nature [11]. This algorithm is a straightforward search method. It includes a set of points rotating around the best point represented as the common center. The SDA's trajectory is characterized by the setting parameters (spiral radius r and rotational angle  $\varphi$ ). It has a good exploitation strategy and a poor exploration strategy when the spiral parameters are set to constant values during the whole search process [12]. For more, the good balance of exploration-exploitation will usually ensure that the global optimality is achieved.

The drawback of all meta-heuristic methods is the premature convergence, which occurs when a trade-off between the exploitation and exploration is not maintained [13]. Much research has been conducted to enhance the performance of these methods, such as hybridizing optimization methods and primarily expanding adaptive methods or incorporating analytical functions into the algorithm [14–17]. In [14], an adaptive version of the spiral dynamics algorithm is presented. The spiral radius parameter is varied using analytical equations and an associated fuzzy logic strategy. Nazir et al. [15] presented a hybrid spiral dynamic bacterial. Hashim et al. [16] enhanced the search diversity of the SDA using a chaotic-maps pattern. In [17], an improved SDA for nonparametric fuzzy logic is presented.

To avoid a risk of premature convergence and enhance

the effectiveness of SDA, this paper proposes an enhancement of SDA named ESDA, where the spiral radius and the rotational angle vary at a dynamic rate following nonlinear functions. This aims to keep the balance between exploration and exploitation strategies.

To highlight the proposed SDA performance, it is compared to GA, PSO, and original SDA with different values of radius and angle from induction motor (IM) parameters identification based on the reference model method [5, 18, 19]. A comparison is established between the ESDA, GA, PSO, and SDAs. The developed programs and the identification approach are verified by using the simulated data, which is obtained for a given machine with known parameters. The assessment is performed on IM's (1.5 kW) parameters estimation.

The rest of the paper is organized in the following order. Section 2 describes a 2-dimensional spiral model for generalization to an n-dimensional spiral model. The original and enhanced SDA are detailed. Section 3 gives the IM model. Section 4 confirms the ESDA performance by the identification method with simulated and measured data. Finally, section 5 draws some conclusions.

# 2. ORIGINAL AND ENHANCED SPIRAL DYNAMIC ALGORITHM

This section presents the 2-dimensional spiral mathematical model, which allows for the introduction of the original SDA. The enhanced SDA is detailed.

# 2.1 A TWO-DIMENSIONAL SPIRAL MATHEMATICAL MODEL

A two-dimensional spiral mathematical model is based on two geometric transformations, as shown in Fig.1.

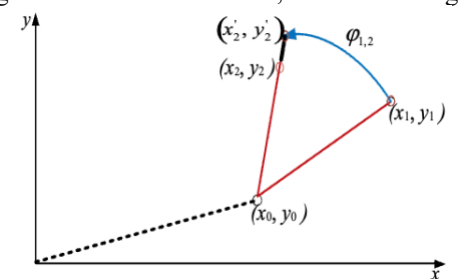


Fig. 1 – Spiral transformation on x-y plane.

The first transformation rotates a point  $(x_1,y_1)^t$ 

Laboratory of Electrical Systems and control LABSET, Faculty of Technology, Saad Dahlab University, BP 270 Soumaa Str., Blida, Algeria. E-mails: boudissa elghalia@univ-blida.dz, Bounekhla.mohamed@cu-tipaza.dz, f.habbi@univ-chlef.dz

442 aaa 2

counterclockwise around the origin point  $(x_0,y_0)^t$  by an angle  $\varphi_{1,2}$ , resulting in another point  $(x_0,y_0)^t$ . This point is then moved to a new position  $(x_0,y_0)^t$  through a homothetic transformation.

The spiral mathematical model can be expressed as follows:

It can be noticed that the point  $(x_0,y_0)^t$  can be given by an identity matrix as below:

$$\begin{pmatrix} x_0 \\ y_0 \end{pmatrix} = \begin{pmatrix} 1 & 0 \\ 0 & 1 \end{pmatrix} \begin{pmatrix} x_0 \\ y_0 \end{pmatrix}. \tag{2}$$

So, the equation (1) can be rewritten as

$${\binom{x_2}{y_2}} = r. \, \mathbf{R}^{(2)} \left( \phi_{1,2} \right) {\binom{x_1}{y_1}} - \left( r. \, \mathbf{R}^{(2)} (\phi_{1,2}) - \mathbf{I} \right) {\binom{x_0}{y_0}}. \tag{3}$$

The rotation matrix is given by

$$\label{eq:R2} \mathbf{R}^{(2)} \big( \phi_{1,2} \big) = \! \begin{pmatrix} \cos\!\phi_{1,2} & -\!\sin\!\phi_{1,2} \\ \!\sin\!\phi_{1,2} & \!\cos\!\phi_{1,2} \end{pmatrix} \!\!.$$

where  $\varphi_{1,2}$  represents the rotation angle around the origin  $(x_0, y_0)^t$ ,  $(0 \le \varphi_{1,2} \le 2\pi)$ . The subscripts of an angle  $\varphi_{1,2}$  indicate the direction of rotation on the x-y plane from point  $(x_1, y_1)^t$  to point  $(x_2', y_2')^t$ , and the sup script of the rotation matrix  $\mathbf{R}^{(2)}$  represents a 2-dimensional orthogonal coordinate system; I represents the identity matrix; r is the homothetic transformation rate, and it is bounded between 0 and 1. The homothetic transformation rate is also named the spiral radius.

# 2.2 ORIGINAL SPIRAL DYNAMIC ALGORITHM (SDA)

Tamura and Yasuda introduced the original SDA [10, 11]. It is a meta-heuristic method based on spiral patterns in nature. Its concept includes a set of points rotating around the best point, defined as the common center, followed by a homothetic transformation for each generation. Therefore, the SDA performance depends on the static setting parameters such as the spiral radius r and the rotational angle. The spiral radius determines the dynamic step size of the spiral trajectory from generation to generation. The rotational angle affects the space between two points in the spiral path and its shape [14]. The SDA mathematical model is obtained by the generalization of a 2-dimensional spiral mathematical model from an *n*-dimensional case given by eq. (4). All points move in a spiral trajectory from one position to a new one.

$$x_{i}(k+1) = r. \mathbf{R}^{(n)}(\varphi_{1,2}, \dots, \varphi_{n-1,n}) x_{i}(k) - -(r. \mathbf{R}^{(n)}(\varphi_{1,2}, \dots, \varphi_{n-1,n}) - I) x_{best}(k).$$
(4)

where  $x_i(k+1)$  is a new position of the  $i^{th}$  point in the  $k^{th}$  iteration;  $x_i(k)$  is the old position of  $i^{th}$  point in the  $k^{th}$  iteration;  $x_{best}(k)$  is the best position in the  $k^{th}$  iteration;  $\mathbf{R}^{(n)}(\phi_{1,2},\phi_{1,3},\phi_{1,4}...,\phi_{n-1,n})$  represents the composition of the rotation matrix,

$$\mathbf{R}^{(n)}(\varphi_{1,2}, \dots, \varphi_{n-1,n}) = \prod_{i=1}^{n-1} \left( \prod_{j=1}^{i} \mathbf{R}_{n-i,n+1-j}^{(n)} (\varphi_{n-i,n+1-j}) \right).$$
(5)

An *n*-dimensional rotation matrix is written as follows:

$$\mathbf{R}^{(n)}(\varphi_{i,j}) = \begin{bmatrix}
1 & \cdots & 0 & 0 & \cdots & 0 & \cdots & 0 \\
\vdots & \ddots & \vdots & & \vdots & \vdots & \vdots & \vdots & \vdots \\
0 & \cdots & 1 & 0 & \cdots & & \cdots & 0 \\
0 & \cdots & \cos\varphi_{i,j} & \cdots & -\sin\varphi_{i,j} & \cdots & 0 \\
\vdots & \vdots & \vdots & \ddots & \vdots & \vdots & \vdots \\
0 & \cdots & 0 & \cdots & 1 & \cdots & 0 \\
\vdots & \vdots & \vdots & \vdots & \ddots & \vdots \\
0 & \cdots & 0 & 0 & \cdots & 0 & 0 & \cdots & 1
\end{bmatrix}, (6)$$

where  $\varphi_{i,j}$  represents the rotational angle in the i-j plane; SDA provides a good exploitation phase because all points are attracted to the best solution. But the exploration phase is poor when the spiral parameters are set to constant values during the whole search process. Then, the trade-off between exploitation and exploration is lost, and premature convergence halts the SDA's success. The following section presents the enhanced SDA, which overcomes the drawback of the original approach.

## 2.3 ENHANCED SPIRAL DYNAMIC ALGORITHM (ESDA)

Initially, the ESDA generates a set of points randomly. The objective function evaluates the fitness value for each point. So, a set of points is rotating around the best point defined as the common center, followed by a homothetic transformation. The setting parameters are modified until the convergence criterion is satisfied. The ESDA proposes the spiral radius and the rotational angle evolving dynamically as the following expressions:

$$r(i) = \begin{cases} r_l, & i \le C_1, \\ A_1(i - C_2)^2 + B_1, & C_1 < i \le C_2, \\ r_u, & i > C_2, \end{cases}$$
(7)

$$\varphi(i) = \begin{cases} \varphi_l, & i \le C_1, \\ A_2(i - C_2)^2 + B_2, & C_1 < i \le C_2, \\ \varphi_u, & i > C_2, \end{cases}$$
(8)

with

$$A_1 = \frac{r_l - r_u}{(c_1 - c_2)^2}.$$

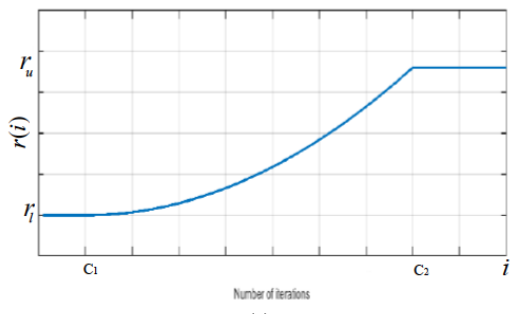
$$B_1 = r_l,$$

$$A_2 = \frac{\varphi_l - \varphi_u}{(c_1 - c_2)^2}.$$

$$B_2 = \varphi_l.$$

i designates the number of iterations;  $r_l, r_u$  represent the variation interval of the spiral radius;  $\varphi_l, \varphi_u$  represent the variation interval of the rotation angles;  $C_1$  designates the starting point of the radius and angle of the proposed functions variation, and  $C_2$  designates the final point of the radius and angle proposed functions variation.

The ESDA aims to foster the abilities of the exploration and exploitation phases to find a global solution. Figure 2 shows the proposed dynamical evolution of the radius and angle according to a nonlinear function. Figure 3 illustrates the flowchart of ESDA.



(a)

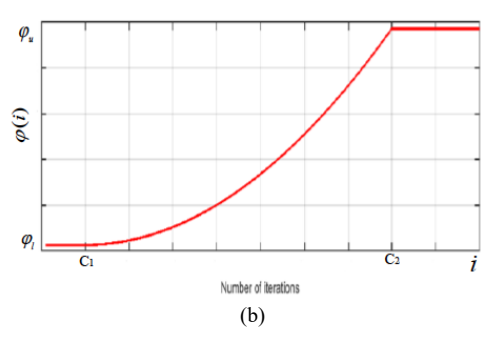


Fig. 2 – The proposed nonlinear functions for: (a) spiral radius; (b) rotational angle.

The nonlinear functions give the exploration phase the possibility of progressing in time and scrutinizing the search space widely while associating itself with a good exploitation phase to achieve the best balance between exploration and exploitation.

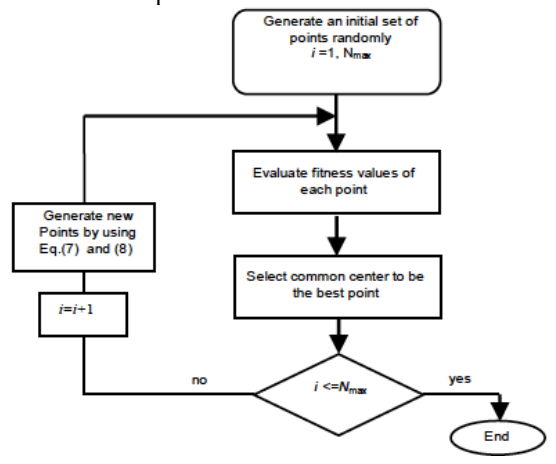


Fig. 3 – Flowchart of the ESDA.

## 3. INDUCTION MACHINE MODEL

The simplifying assumptions for establishing a dynamic model of IM are summarized as follows:

- Neglected saturation effect
- Neglected core losses
- Neglected skin effect
- Limitation to the first space harmonic
- Constant air gap

The IM equations [20] related to a reference linked to the stator are given by:

$$\begin{cases} \frac{\mathrm{d} I_{qs}}{\mathrm{d}t} = -\frac{1-\sigma}{\sigma} P_0 \Omega I_{ds} - \frac{1}{\sigma T_s} I_{qs} - \frac{1-\sigma}{\sigma} P_0 \Omega I'_{dr} + \frac{1-\sigma}{\sigma T_r} I'_{qr} + \frac{v_{qs}}{\sigma L_s}, \\ \frac{\mathrm{d} I'_{dr}}{\mathrm{d}t} = \frac{1}{\sigma T_s} I_{ds} - \frac{1}{\sigma} P_0 \Omega I_{qs} - \frac{1}{\sigma T_r} I'_{dr} - \frac{1}{\sigma} P_0 \Omega . I'_{qr} - \frac{v_{ds}}{\sigma L_s}, \\ \frac{\mathrm{d} I_{ds}}{\mathrm{d}t} = -\frac{1}{\sigma T_s} I_{ds} + \frac{1-\sigma}{\sigma} P_0 \Omega I_{qs} + \frac{1-\sigma}{\sigma T_r} I'_{dr} + \frac{1-\sigma}{\sigma} P_0 \Omega I'_{qr} + \frac{v_{ds}}{\sigma L_s}, \\ \frac{\mathrm{d} I'_{qr}}{\mathrm{d}t} = \frac{1}{\sigma} P_0 \Omega I_{ds} + \frac{1}{\sigma T_s} I_{qs} + \frac{1}{\sigma} P_0 \Omega I'_{dr} - \frac{1}{\sigma T_r} I'_{qr} - \frac{v_{qs}}{\sigma L_s}, \\ \frac{\mathrm{d} \Omega}{\mathrm{d}t} = \frac{1}{J} (1-\sigma) L_s (I_{qs} I'_{dr} - I_{ds} I'_{qr}) - \frac{B\Omega}{J}. \end{cases}$$

where:

$$\sigma = 1 - \frac{L_m^2}{L_s L_r}, \quad T_r = \frac{L_r}{R_r}, \quad T_s = \frac{L_s}{R_s},$$
 (10)

and  $P = [\sigma, T_r L_s T_s J B]^T$  represents the parameter vector.

This vector is determined using only the measured current and the corresponding phase voltage, applied to the motor of a transient from standstill to steady state operation.

#### 4. RESULTS

To highlight the performance of the SDAs and ESDA, they are applied to perform, at the same time, the electrical and mechanical parameters of the IM. Then, the quadratic error S is minimized by the SDAs and ESDA.

$$S = \sum_{i=1}^{n} (I_{mi} - I_{ci})^{2}, \tag{11}$$

where  $I_{mi}$  is the measured current and  $I_{ci}$  is the computed current. The above developed algorithms' performances are tested using both simulated and measured data for the identification method [5].

#### 4.1 SIMULATED DATA

The developed program and identification approach are verified by using the simulated data, which is obtained for a given IM with known parameters and fed with a sine voltage. The simulated data are computed from the system (9) with the fourth-order Runge-Kutta method. The data are given by the sinusoidal voltage supply and the corresponding calculated current (Fig. 4).

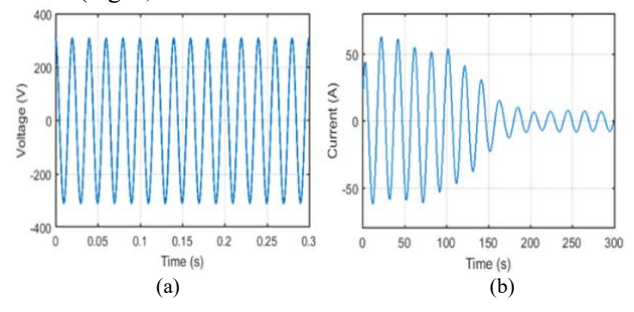


Fig. 4 – (a) Voltage supply; (b) Calculated stator current.

Table 1 summarizes the setting parameters of ESDA and SDAs for different spiral radius and rotational angle values.

Table 1

ESDA and SDAs setting parameters for simulated data

Algorithms	Radius and angle	Set of points	Maximum number of iterations
ESDA1	$ \begin{bmatrix} [r_i, \theta_i] = [0.85, \ \pi/3] \\ [r_u, \theta_{ul}] = [0.95, \ \pi/2] \\ [C_1, C_2] = [15, 80] $	200	100
SDA1	$[r,\theta] = [0.95, \pi/4]$	200	100
SDA2	$[r, \theta] = [0.98, \pi/2]$	200	100
SDA3	$[r,\theta] = [0.85, \pi/5]$	200	100

The parameter identification results using SDA1, SDA2, SDA3, ESDA1, GA, and PSO are given in Table 2.

Table 2
Results of simulated parameters.

Parameters	Given parameters	ESDA1	SDA1	SDA2	SDA3	GA	PSO
σ	0.09	0.09	0.032	0.033	0.033	0.029	0.089
Tr (ms)	123	122.9	451.53	340.71	343.65	375.45	123.23
Ts (ms)	159	158.9	422.17	383.65	452.14	488.93	159.21
Ls (mH)	0.054	0.054	0.142	0.123	0.203	0.173	0.054
$J(kg.m^2)$	0.038	0.038	0.033	0.037	0.041	0.042	0.038
B (N.m.s/Rd)	0.001	0.001	0.007	0.015	0.045	0.001	0.001

By the ESDA1, the estimated parameters are very close to the given parameters, as shown in Table 2. Then, the convergence of ESDA1 and PSO is confirmed. But the estimated electrical parameters by SDA1, SDA2, SDA3, and GA are far from the given parameters. When their estimated mechanical parameters are near the given parameters. Consequently, the results showed premature convergence of SDA1, SDA2, SDA3, and GA, with all being trapped in local minima. Figure 5 (a-f) illustrates the estimated

parameters' evolution versus the number of iterations.

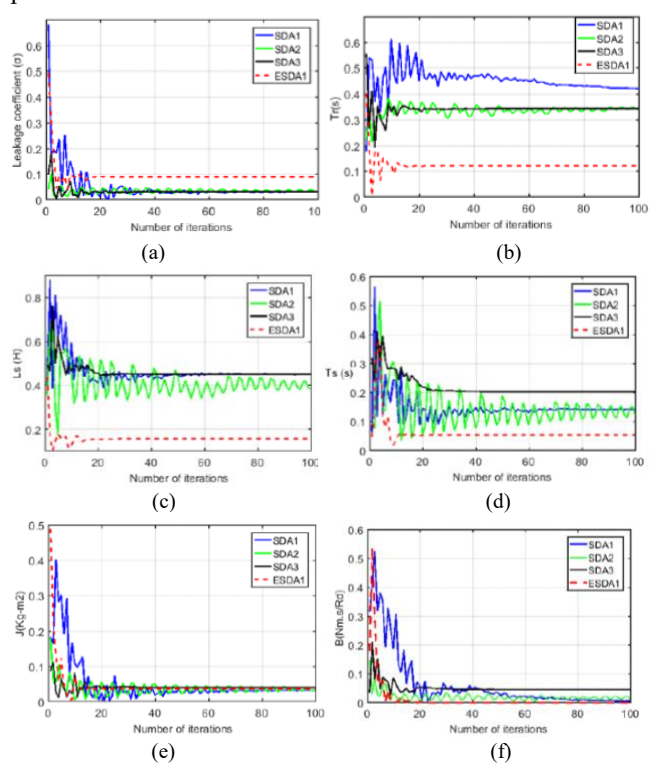


Fig. 5 – Estimated parameters evolution by SDA1, SDA2, SDA3, ESDA1, GA, and PSO.

The estimated parameters evolution confirms the convergence of the ESDA1 and PSO, with the premature convergence of the SDA1, SDA2, SDA3, and GA. It can be noticed that the convergence of ESDA1 and PSO started from the 20<sup>th</sup> and 80<sup>th</sup> iteration, respectively. Then, the ESDA1 performance shows high convergence speed.

#### 4.2 MEASURED DATA

Tests are performed on motor M, characterized by 4 poles, 220/380 V, and 1.5 kW. The current and the phase voltage given in Fig.7 are simultaneously measured using the experimental setup given in Fig. 6.

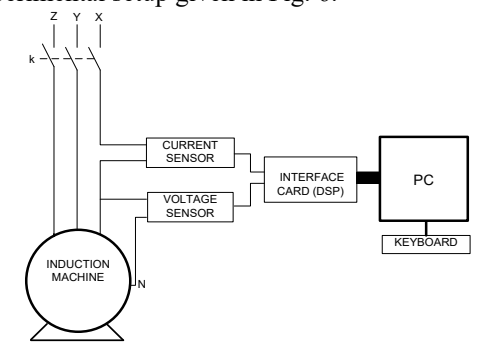


Fig. 6 – Measurement setup.

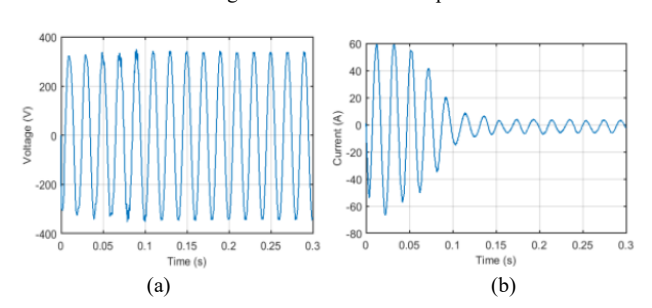


Fig. 7 - Motor M; (a) Measured voltage; (b) Measured current.

A motor parameters estimation method is based on the developed programs of ESDA and SDAs with different values of radius and angle given in Table 3.

Table3
ESDA and SDAs setting parameters for measured data.

Algorithms	Radius and angle	Set of	Maximum number
		points	of iterations
ESDA2	$[r_l, \theta_l] = [0.8, \pi/5]$	200	100
	$[r_u, \theta_u] = [0.98, \pi/2]$		
	$[C_1, C_2] = [10, 80]$		
SDA1	$[r,\theta] = [0.95, \pi/4]$	200	100
SDA2	$[r, \theta] = [0.98, \pi/2]$	200	100
SDA4	$[r,\theta] = [0.8, \pi/5]$	200	100

Using the measured data, the estimated parameters for motor M are given in Table 4.

Table 4
Estimated parameters.

Parameters	ESDA2	SDA1	SDA2	SDA4	GA	PSO
σ	0.069	0.072	0.0265	0.0209	0.024	0.069
Tr (ms)	135.15	129.18	285.81	502.18	422.31	134.19
Ts (ms)	189.55	182.43	535.21	586.64	560.38	188.82
Ls (mH	87.21	83.58	38.14	31.14	26.33	87.01
J (kg.m <sup>2</sup> )	0.0353	0.0350	0.0107	0.0083	0.0362	0.0354
B (N.m.s/Rd)	0.0097	0.0102	0.0053	0.0028	0.0092	0.0097

The estimated parameters evaluation is carried out using the comparison by superposition between the calculated current and the measured one. This evaluation shows the algorithm convergence. The estimated parameters represent the minimum of the quadratic output error between the measured and computed currents. The computed current is acquired by numerical resolution of the nonlinear system (9) by means of the fourth-order Runge-Kutta method using the estimated parameters given in Table 4.

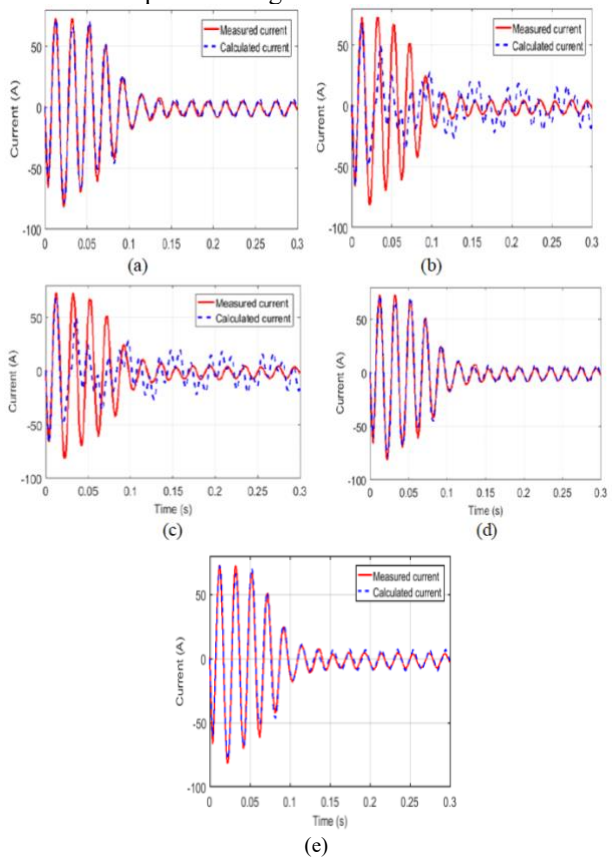


Fig. 8 – Superposition of the measured current and calculated one with the estimated parameters to motor M; (a) ESDA2; (b) SDA4; (c) SDA2; (d) SDA1; (e) by PSO, by GA.

Figure 8 illustrates the matching of the measured current and the computed one with the identified parameters by ESDA2, SDA1, SDA2, SDA4, GA, and PSO for motor M. It allows us to show the convergence when the measured current and the computed one agree well in transient and steady states. Moreover, Fig. 8 shows the best matching of curves related to ESDA2 and SDA4 to ensure their convergence.

About GA, the curve doesn't match in the steady state only. But the curves related to SDA2 and SDA4 don't agree well in the transient and steady state, and they are trapped in a local minimum. Also, the parameter variation versus the number of iterations for motor M, illustrated in Fig. 9, confirms the speed convergence.

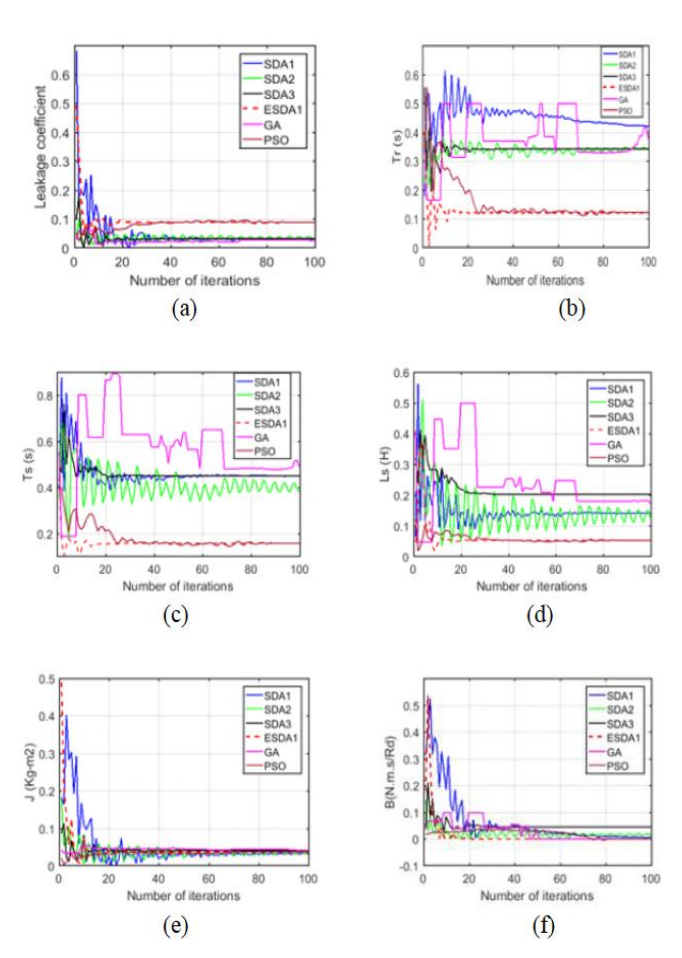


Fig. 9 – Parameters evolution of motor M; (a) of the leakage coefficient; (b) of Tr; (c) of Ls; (d) of Ts; (e) of J; (f) of B

The estimated parameters evolution confirms the convergence of the ESDA2, PSO, and SDA1. It can be noticed that the convergence of ESDA2, PSO, and SDA1 started from the 15<sup>th</sup>, 40<sup>th</sup>, and 80<sup>th</sup> iteration, respectively. Then, the ESDA2 performance shows a higher convergence speed than SDA1 and PSO, where SDA2 and SDA4 are stuck in a local minimum.

# 4.3 STATISTICAL STUDY

Each algorithm is executed 10 times. As a termination criterion, the maximum number of iterations is considered, which has been set to 100. In all simulations, the population size has been configured to 200.

To evaluate the performance of all algorithms, the statistical results are presented in Table 5 for the given IM, including the mean and standard deviation of fitness values.

Table 5
Simulated results obtained by GA, PSO, SDA1, SDA2, SDA3, and ESDA1using fitness values.

Algorithms	Mean	Standard deviation
GA	1.322369557603000e+03	7.236734422254997e+02
PSO	55.145737770000004	84.733397754501425
SDA1	3.935917006284000e+03	2.911851558895321e+03
SDA2	1.411874686054546e+03	1.212562445739074e+03
SDA3	5.928601770146000e+03	4.563489867739208e+03
ESDA1	54.880410530999995	62.554968601056878

The ESDA1 had the lowest standard deviation of 62.554968601056878, resulting in robust performance among the algorithms. The standard deviation and mean comparisons are depicted in Fig. 10 (a, b).

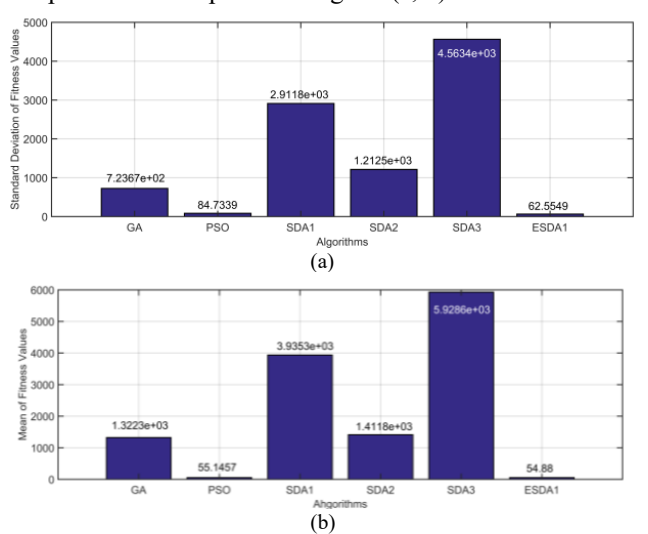


Fig. 10 – Standard deviation comparison of algorithms (a) Mean comparison of algorithms (b).

# 6. CONCLUSIONS

This paper proposes an enhancement of SDA named ESDA, where the spiral radius and the rotational angle vary at a dynamic rate following nonlinear functions. This aims to realize the trade-off between the exploration and the exploitation phases. To highlight the ESDA performance, it is compared to GA, PSO, and original SDA with different values of radius and angle from IM parameters identification. So, these parameters are determined simultaneously from the measured current and the corresponding phase voltage. This procedure uses the reference model method and relies on the SDAs, ESDA, GA, and PSO as a minimization technique.

Based on simulated data, the results obtained from the ESDA1 have shown that this method can be successfully applied to identify the model parameters with a high degree of accuracy. The convergence of ESDA1 and PSO started from the 20th and 80th iteration, respectively. The results also show that ESDA1 converges to an optimal solution much more quickly than PSO, whereas ESDA2 and ESDA3 are trapped in local minima.

Using measured data, the convergence of ESDA2, PSO, and SDA1 started from the 15<sup>th</sup>, 40<sup>th</sup>, and 80<sup>th</sup> iteration, respectively. The ESDA2 performance shows higher convergence speed than SDA1 and PSO, where SDA2, GA, and SDA4 converge prematurely. The simulated and measured data demonstrate that the proposed SDA shows the best optimization effectiveness compared to GA, PSO and the original SDAs in term of convergence speed.

446 aaa 6

#### CREDIT AUTHORSHIP CONTRIBUTION

Author 1: conceptualization, software, validation, writing

Author\_2: methodology, writing Author\_3: software, formal analysis

# NOMENCLATURE

NOWENCEATORE							
$V_{dr}$ , $V_{qr}$	d-q axes rotor voltage	В	viscous friction coefficient				
$V_{ds}$ , $V_{qs}$	d-q axes stator voltage		(N.m.s/Rd)				
$I_{dr}$ , $I_{qr}$	d-q axes rotor current	σ	leakage coefficient				
$I_{ds}$ , $I_{qs}$	d-q axes stator current	$T_r$	rotor time constant (s)				
$R_s$ , $R_r$	stator and rotor	$T_s$	stator time constant (s)				
	resistances $(\Omega)$	$P_o$	number of pole pairs				
Ω	mechanical velocity						
	(Rd/s)						
$L_m$	mutual inductance (H)						
$L_s$ , $L_r$	stator and rotor						
	inductances (H)						
J	rotor inertia (kg.m <sup>2</sup> )						

# Received on 12 February 2025

#### REFERENCES

- Hanif Halim, I. Ismail, and D. Swagatam, Performance assessment of the metaheuristic optimization algorithms: an exhaustive review, Artificial Intelligence Review, 54, 3, pp. 2323–2409 (2021).
- K. Satnam, K.A. Lalit, A.L. Sangal, and D. Gauravn, Tunicate swarm algorithm: a new bio-inspired based metaheuristic paradigm for global optimization, Engineering Applications of Artificial Intelligence, 90 (2020).
- 3. S. Ekinci, D. Izci, and L. Abualigah, A novel balanced Aquila optimizer using random learning and Nelder-Mead simplex search mechanisms for air-fuel ratio system control, J Braz. Soc. Mech. Sci. Eng., 45, 68 (2023).
- D. Izei, B. Hekimoglu, and S. Ekinci, A new artificial ecosystembased optimization integrated with Nelder-Mead method for PID controller design of buck converter, Alexandria Engineering Journal, 61, pp. 2030–2044 (2022).
- E. Boudissa, F. Habbi, N.E.H. Gabour, and M. Bounekhla, A new dynamic genetic selection algorithm: application to induction machine identification, Rev. Roum. Sci. Techn. Électrotechn. Et Énerg., 66, 3, pp. 145–151 (2021).
- D. Naas, E. Boudissa, M. Bounekhla, and I. Dif, Firefly algorithm improvement with application to induction machine, Rev. Roum. Sci. Techn. – Électrotechn. Et Énerg., 65, 1, pp. 35–40 (2020).
- A.S.A. Bayoumi, R.A. El Sehiemy, and A. Abaza, Effective PV
  parameter estimation algorithm based on marine predators
  optimizer considering normal and low radiation operating

- conditions, Arabian Journal for Science and Engineering (2021).
- A.A. Mekki, A. Kansab, M. Matallah, and M. Feliachi, Optimization
  of the inductor of an induction cooking system using particle
  swarm optimization method and fuzzy logic controller, Rev.
  Roum. Sci. Techn. Électrotechn. Et Énerg., 65, 3–4, pp. 185–
  190 (2020).
- X. Jianzhong and F. YanBisht, Effective PV parameter estimation algorithm based on marine predators optimizer considering normal and low radiation operating conditions, Arabian Journal for Science and Engineering (2019).
- K. Tamura and K. Yasuda, Primary study of spiral dynamics inspired optimization, IEEJ Trans Electric Electron Eng., 6, pp. 98–100 (2011).
- K. Tamura and K. Yasuda, Spiral dynamics inspired optimization, J Adv Comput Intell Inform, 15, 8, pp. 1116–1122 (2011).
- A.N.K. Nasir and M.O. Tokhi, Novel metaheuristic hybrid spiraldynamic bacteria-chemotaxis algorithms for global optimisation, Applied Soft Computing, 27, pp. 357–375 (2015).
- E. Cuevas, A. Echavarría, and M.A. Ramírez-Ortegón, An optimization algorithm inspired by the States of Matter that improves the balance between exploration and exploitation, Applied Intelligence, 40, pp. 256–272 (2014).
- A.N.K. Nasir, M.O. Tokhi, N.M. Abd Ghani, and R.M.T. Raja Ismail, Novel adaptive spiral dynamics algorithms for global optimization, In Proceedings of the 2012 IEEE 11th International Conference on Cybernetic Intelligent Systems (CIS), Guildford, UK, pp. 99–104 (2012).
- A.N.K. Nasir, M.O. Tokhi, N.M. Abd Ghani, and M.A. Ahmad, A novel hybrid spiral-dynamics bacterial-foraging algorithm for global optimization with application to control design, In 2012 12th UK Workshop on Computational Intelligence (UKCI), pp. 1–7 (2012).
- M.R. Hashim and M.O. Tokhi, Chaotic spiral dynamic optimization algorithm, In 19th International Conference on Climbing and Walking Robots and the Support Technologies for Mobile Machines, London, UK, pp. 1–8 (2016).
- 17. A.N.K. Nasir and M.O. Tokhi, *An improved spiral dynamic optimization algorithm with engineering application*, IEEE Trans. Syst. Man. Cybern. Syst., **45**, pp. 943–954 (2015).
- A. Accetta, F. Alonge, M. Cirrincione, M. Pucci, and A. Sferlazza, Parameter identification of induction motor model by means of state space-vector model output error minimization, In XXI International Conference on Electrical Machines (ICEM), pp. 843–849 (2014).
- J.W. Rengifo-Santana, J. Benzaquen-Suñe, J.M. Aller-Castro, A.A. Bueno-Montilla, and A. Restrepo-Zambrano, *Parameter estimation method for induction machines using instantaneous voltage and current measurements*, Rev. Fac. Ing. Univ. Antioquia, 75, pp. 57–66 (2015).
- J. Chatelain, Machines électriques, In Traité d'Électricité, Vol. X, Lausanne, France: Presses Polytechniques Romandes (1983).